

First-principles study on lithium borohydride LiBH₄

Kazutoshi Miwa,* Nobuko Ohba, and Shin-ichi Towata

Toyota Central Research & Development Laboratories, Inc., Nagakute, Aichi 480-1192, Japan

Yuko Nakamori and Shin-ichi Orimo

Institute for Materials Research, Tohoku University, Sendai 980-8577, Japan

(Received 27 January 2004; published 30 June 2004)

First-principles calculations have been performed on lithium borohydride LiBH₄ using the ultrasoft pseudopotential method, which is a potential candidate for hydrogen storage materials due to its extremely large gravimetric capacity of 18 mass % hydrogen. We focus on an orthorhombic phase observed at ambient conditions and predict its fundamental properties; the structural properties, electronic properties, dielectric properties, vibrational properties, and the heat of formation. The calculation gives a nearly ideal tetrahedral shape for BH₄ complexes, although the recent experiment suggests that their configuration is strongly distorted [J-Ph. Soulié *et al.*, *J. Alloys Compd.* **346**, 200 (2002)]. Analyses for the electronic structure and the Born effective charge tensors indicate that Li atoms are ionized as Li⁺ cations. The internal bonding of [BH₄]⁻ anions is primarily covalent. The high-frequency dielectric permittivity tensor ϵ_{∞} is predicted as almost isotropic, but the static dielectric permittivity tensor ϵ_0 as considerably anisotropic. The Γ -phonon eigenmodes can be classified into three groups, namely, the librational modes involving the displacements of Li⁺ cations (less than 500 cm⁻¹), and the internal B-H bending and stretching modes of [BH₄]⁻ anions (around 1100 and 2300 cm⁻¹, respectively). The molecular approximation fairly reproduces the phonon frequencies in the latter two groups, implying the strong internal bonding of BH₄ complexes. The librational modes have significant contributions to the large anisotropies of ϵ_0 . The agreement of the heat of formation with the experimental value is reasonably good.

DOI: 10.1103/PhysRevB.69.245120

PACS number(s): 71.20.Ps, 61.66.Fn, 77.22.-d, 63.20.Dj

I. INTRODUCTION

Alkali complex hydrides have attracted growing interest due to their high gravimetric densities of hydrogen for hydrogen storage materials. Bogdanović and Schwickardi have reported that the catalyzed sodium alanate (NaAlH₄) shows reversible hydriding and dehydriding reactions at moderate temperatures.¹ Motivated by this report, many attempts have been tried to enhance the reversibility of the hydriding/dehydriding reactions for alkali complex hydrides.²⁻¹⁰

Among alkali complex hydrides, lithium borohydride LiBH₄ is a potential candidate¹¹ because of its extremely high hydrogen content of 18 mass %. This material is, however, rather stable and desorbs hydrogen only at elevated temperatures, above the melting point of about 540 K. The dehydriding reaction is caused by the decomposition of LiBH₄ into LiH and B. A synthesis of LiBH₄ from the elements has not been reported yet and it is expected to require extremely elevated conditions. In order to improve the performance, the understanding of the basic material properties is of great interest.

The crystal structures of LiBH₄ have been studied by synchrotron x-ray powder diffraction.¹² At ambient conditions, LiBH₄ has orthorhombic symmetry with space group *Pnma*. At high temperature (~381 K), the compound undergoes a phase transition to a hexagonal structure with space group *P6₃mc*. As shown in Fig. 1, four hydrogen atoms are arranged around a boron atom in a tetrahedral configuration in both structures.

The experimental results^{11,12} suggest that the BH₄ complexes in the orthorhombic phase are strongly distorted from an ideal tetrahedral geometry.

Theoretical investigations using the first-principles calculations are not so common for alkali complex hydrides and only few studies have been reported.^{13,14} In addition, the previous studies are mainly concerned with alanates and no detailed theoretical investigations have been carried out for LiBH₄. In this paper, we perform the first-principles calculations on LiBH₄ to predict its fundamental properties; the structural properties, electronic properties, dielectric properties, vibrational properties, and heat of formation. This study is restricted to the orthorhombic phase observed at ambient conditions and only a brief discussion is presented for the hexagonal phase.

II. METHOD

The present calculations have been performed using the ultrasoft pseudopotential method¹⁵ based on density functional theory.¹⁶ The generalized gradient approximation proposed by Perdew, Burke, and Ernzerhof¹⁷ is used for the exchange-correlation energy.

All pseudopotentials are constructed from the results of scalar-relativistic all-electron calculations.¹⁸ The pseudowave functions and the pseudoaugmentation charge functions are optimized by the method similar to that proposed by Rappe *et al.*¹⁹ For hydrogen, the pseudopotential is constructed for the 1*s* state using double projector functions and the 2*p* state is treated as the local part of the pseudopotential. For Li and B, the 2*s* and 2*p* states are chosen as the reference states and the 3*d* state as the local part of pseudopotential, where a single projector function is employed for each com-

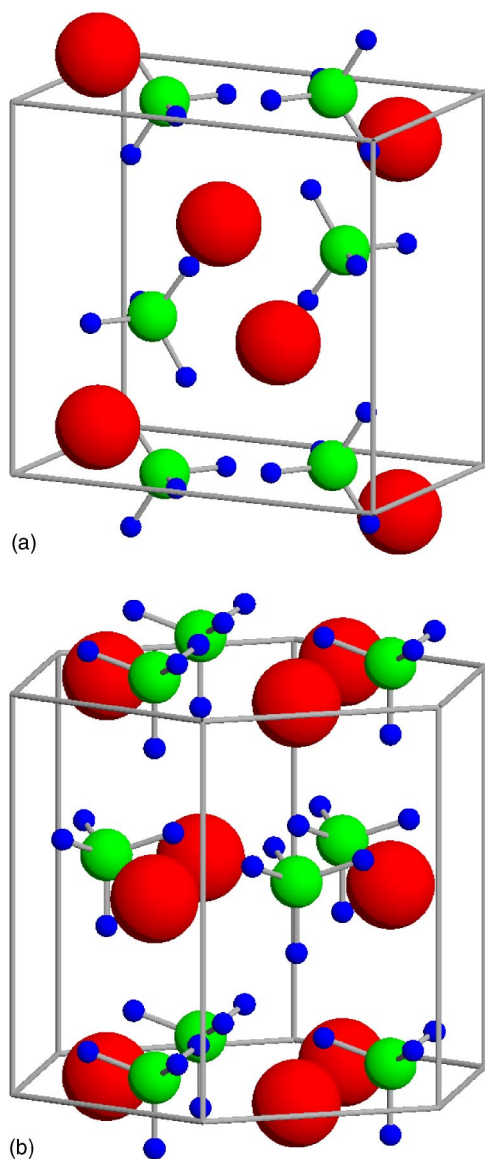


FIG. 1. (Color online) Crystal structures of LiBH₄ in (a) orthorhombic phase at room temperature and (b) hexagonal phase at high temperature. Red (large), green (middle), and blue (small) spheres represent Li, B, and H atoms, respectively.

ponent, and the partial core correction²⁰ is adopted. For Li, the norm-conserving condition²¹ is imposed to enhance the efficiency of calculations. In the solid-state calculations, the Kohn-Sham equation is solved by the iterative diagonalization scheme.²² The details of computational procedure for the self-consistent-field calculation and the structural relaxation can be found in Refs. 22 and 23.

The dielectric properties have been calculated within the framework of the self-consistent density-functional perturbation theory (DFPT).^{24,25} The macroscopic high-frequency dielectric permittivity tensor is related to the second derivative of the total energy with respect to external electric field, which contains only the contribution of the electronic polarization. The Born effective charge tensor is formulated by the mixed second derivative with respect to external electric field and atomic displacements. Knowledge of these proper-

ties is essential for describing the long-range dipolar contribution to the lattice dynamics of a polar crystal. The Born effective charge tensor is also useful to consider the bonding character of materials. The details of the linear response calculation within the ultrasoft pseudopotential method and DFPT can be found in Ref. 24.

The phonon eigenmodes are obtained by solving the eigenvalue problem for the dynamical matrix which is calculated by the force-constant method.²⁶ The atomic displacement is set to be 0.02 Å. At the Γ point, the infrared active modes are divided into the transverse optical (TO) modes and the longitudinal optical (LO) modes. In this case, the dynamical matrix must be modified by adding the dipole-dipole interactions induced by the atomic displacements. This term is completely defined from the knowledge of the macroscopic high-frequency dielectric permittivity tensor and the Born effective charge tensors, from which the macroscopic low-frequency dielectric permittivity tensor can also be obtained by combining with the knowledge of the eigenvectors and eigenvalues for the bare dynamical matrix.²⁵

To examine the transferability of the pseudopotentials, the calculations have been performed on the related solids Li, B, and LiH and a hydrogen molecule. We choose the metastable α phase of B for simplicity. The cutoff energies used here are 15 and 120 hartrees for the pseudowave functions and the charge density, respectively. For the solids, the k -point grids for the Brillouin zone integration are generated so as to make the edge lengths of the grid elements closer to the target value of 0.08 bohr⁻¹ as possible. The same conditions are applied for the calculations on LiBH₄. The resulting k -point grids are $6 \times 10 \times 6$ and $12 \times 12 \times 6$ for the orthorhombic and hexagonal phases, respectively. We have checked that these conditions give good convergence of the total energy within 1 meV/atom. The calculation for a hydrogen molecule is carried out using a cubic supercell with size of $8 \times 8 \times 8$ Å³ with the single Γ point for the k -point sampling. The zero-point energies are obtained within the harmonic approximation, where the phonon densities of state are calculated with the supercells containing 64, 72, and 64 atoms for Li, B, and LiH, respectively. The results are given in Table I.

The lattice constants (interatomic distance) and the cohesive energies are in good agreement with the available experimental data. The agreement of the atomic positions in α -B is also good.³⁰ The zero-point energies are important to predict the heat of formation related to the hydriding/dehydriding reaction²³ though these energies have only small fractions in the cohesive energies.

III. RESULTS AND DISCUSSION

A. Structural properties

First, the lattice constants are kept fixed at the experimental values and the atomic configuration is only relaxed. Table II shows the result of the calculation, together with the experimental data obtained from synchrotron x-ray powder diffraction by Soulié *et al.*¹² The energy gain of the atomic relaxation from the experimental configuration is

TABLE I. Results for bcc-Li, α -B, H₂ molecule, and NaCl-type LiH. Lattice constants a and c (Å), cohesive energy E_{coh} (eV/atom), interatomic distance d (Å), and zero-point energy E_{zero} (meV/atom). Note that the zero-point energies are not included in E_{coh} .

	Property	Present	Experiment
bcc-Li	a	3.444	3.491 ^a
	E_{coh}	1.61	1.63 ^a
	E_{zero}	40	
α -B	a	4.947	4.91 ^b
	c	12.674	12.57 ^b
	E_{coh}	6.20	
	E_{zero}	126	
H ₂	d	0.756	0.741 ^c
	E_{coh}	2.27	2.37 ^c
	E_{zero}	135	
LiH	a	3.987	4.083 ^c
	E_{coh}	2.36	
	E_{zero}	111	

^aReference 27.

^bReference 28.

^cReference 29.

0.92 eV/formula unit. Although the agreement between the predicted structural parameters and the experimental ones is fairly good for Li and B, some discrepancies are found for H. For clear comparison, we summarize the bond lengths and the bond angles of tetrahedral BH₄ complexes in Table III.

The calculation predicts a nearly ideal tetrahedral shape where the bond lengths are almost constant and the bond angles are close to the ideal value $\theta_{\text{H-B-H}}=109.5^\circ$. This contradicts the experimental result that BH₄ complexes are strongly distorted with respect to bond lengths and bond angles.

To check this problem, we repeat the structural optimization in which both the lattice constants and the atomic positions are allowed to relax. The obtained lattice constants are $a=7.343$ Å, $b=4.399$ Å, and $c=6.588$ Å: The deviation from the experimental values is 2, -1, and -3 %, respectively. The energy gain of this relaxation is only 3.8 meV/formula unit. The bond lengths and the bond angles of BH₄ complexes are 1.23–1.24 Å and 108°–111°, respec-

TABLE III. Bond lengths, $d_{\text{B-H}}$ (Å), and bond angles, $\theta_{\text{H-B-H}}$ (deg.) of BH₄ complexes in orthorhombic LiBH₄.

	$d_{\text{B-H}}$	$\theta_{\text{H-B-H}}$
Present	1.23–1.24	108–111
Experiment ^a	1.04–1.28	85–120

^aReference 12.

tively. The shape of BH₄ complexes is hardly changed by the lattice relaxation and retains an ideal configuration. The calculations cannot reproduce the distorted geometry for BH₄ complexes observed experimentally. The reason of this discrepancy is unclear and more detailed investigation is required. Züttel *et al.*¹¹ have also reported a strongly deformed configuration. However, the obtained bond lengths are 1.28–1.44 Å, which are in poor agreement with those of Soulié *et al.* Very recently, Noritake *et al.*³¹ have also performed the structural analysis for LiBH₄ by synchrotron x-ray powder diffraction. Their results are somewhat close to our prediction. The existence of various sets of experimental data may indicate that the discrepancies are caused by the experimental difficulties in identifying hydrogen positions due to their weak x-ray scattering power.

In the following sections, the structural parameters obtained using the experimental lattice constants are used. We can expect that the lattice relaxation gives only minor effects because the amount of the relaxation is small and the geometry of BH₄ complexes which are basic units of LiBH₄ are essentially unchanged.

B. Electronic properties

Figure 2 depicts the total and partial densities of states for LiBH₄. The electronic structure is nonmetallic with the calculated energy gap of 6.8 eV. Because there is little contribution of Li orbitals to the occupied states, Li atoms are thought to be ionized as Li⁺ cations. The occupied states split into two peaks: The low-energy states are composed of B-2s and H-1s orbitals and the high-energy states consist of B-2p and H-1s orbitals. These bonding properties are similar to those of a CH₄ molecule. A boron atom constructs sp^3 hybrids and forms covalent bonds with surrounding four H atoms. A deficient electron to form these bonds is compensated by a Li⁺ cation.

TABLE II. Structural parameters of orthorhombic LiBH₄. Space group: $Pnma$ (No. 62). The lattice constants are fixed at the experimental values $a=7.179$ Å, $b=4.437$ Å, and $c=6.803$ Å.

Atom	Site	Present			Experiment ^a		
		x	y	z	x	y	z
Li	4c	0.1552	1/4	0.1137	0.1568	1/4	0.1015
B	4c	0.3141	1/4	0.4229	0.3040	1/4	0.4305
H1	4c	0.9131	1/4	0.9263	0.900	1/4	0.956
H2	4c	0.4061	1/4	0.2656	0.404	1/4	0.280
H3	8d	0.2145	0.0246	0.4224	0.172	0.054	0.428

^aReference 12.

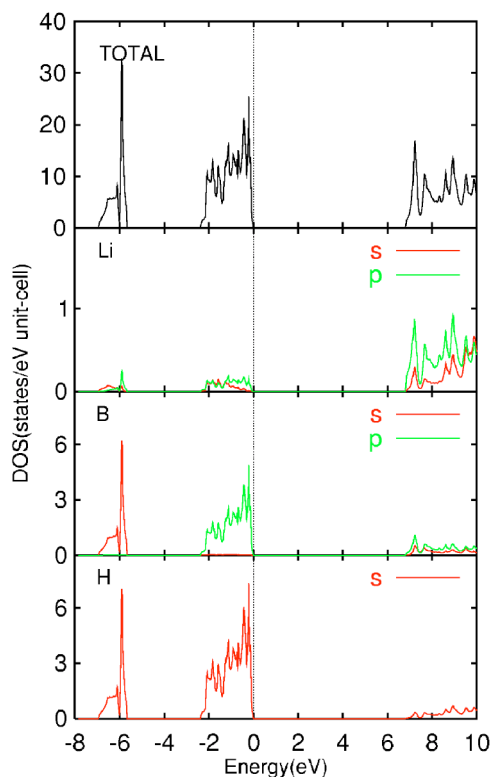


FIG. 2. (Color online) Total and partial densities of states for orthorhombic LiBH_4 . The origin of the energy is set to be the top of valence states.

The valence charge contour plot is shown in Fig. 3. As expected, the charge density around Li is considerably low. The valence charge density is strongly localized around BH_4 complexes and no overlaps between them are observed. This indicates that the interaction between BH_4 complexes is weak, which coincides with the fact that the band widths of the occupied states are relatively narrow.

C. Dielectric properties

The results of the dielectric properties for LiBH_4 are listed in Table IV. The macroscopic high-frequency dielec-

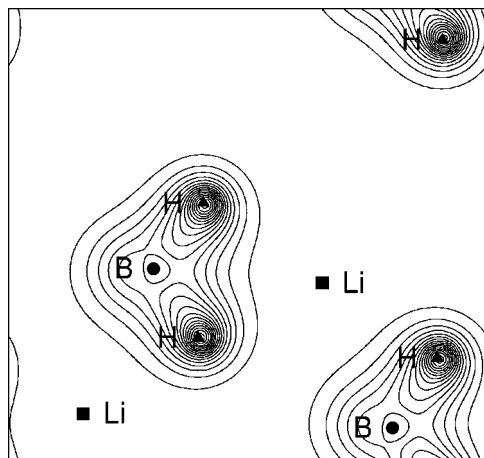


FIG. 3. Valence charge contour plot for orthorhombic LiBH_4 in the (010) plane. The contour spacing is $0.02 e/\text{bohr}^3$.

tric permittivity tensor ϵ_∞ is diagonal due to the crystal symmetry. The diagonal elements of ϵ_∞ are almost same and so the anisotropies of ϵ_∞ are small. Since ϵ_∞ contains only the contribution from the electronic polarization, it is expected that the contribution of the occupied states localized around BH_4 complexes is dominant compared with that of empty Li orbitals. The nearly ideal tetrahedral configuration of BH_4 complexes will reflect the small anisotropies of ϵ_∞ . The macroscopic low-frequency dielectric permittivity tensor ϵ_0 , which is also diagonal, can be obtained by adding to ϵ_∞ the ionic contribution. Unlike ϵ_∞ , the considerable anisotropies are found for ϵ_0 . These anisotropies are caused by the phonon eigenmodes involving Li displacements, which will be discussed in the next section.

The Born effective charge tensors Z^* obtained in this study satisfy the acoustic sum rule²⁵ with an error of less than $0.01 e/\text{atom}$. Because of the site symmetries, four off-diagonal elements are equal to zero except for H3 (see Table II) for which all elements are finite values. The diagonal elements of Z^*_{Li} are close to the expected value of +1 and absolute values of the off-diagonal elements are relatively small. This supports an ionic picture for Li described in the previous section. Considering the acoustic sum rule, BH_4 complexes are thought to be ionized as $[\text{BH}_4]^-$ anions. For B and H atoms, absolute values of all elements are small, and so few ionic characters are extractable for the internal bonding of BH_4 complexes: Although H atoms seem to be negatively charged slightly, it is inadequate to expect the mixed ionic bonding, i.e., $\text{Li}^+\text{B}^{3+}\text{H}_4^-$, which has been recently proposed for NaAlH_4 .³² As mentioned in the previous section, the internal bonding of BH_4 complexes is primarily covalent.

D. Vibrational properties at Γ point

The vibrational properties are most accessible to experimental probes at the Γ point. Since the unit cell contains four formula units, there are 69 optical Γ -phonon modes. The irreducible representation of them is $11A_g + 7B_{1g} + 11B_{2g} + 7B_{3g} + 7A_u + 10B_{1u} + 6B_{2u} + 10B_{3u}$; all *gerade* modes are Raman active, $7A_u$ modes are inactive, and other *ungerade* modes are infrared active. The calculated phonon frequencies are given in Table V.

Our Raman spectroscopy measurements³³ give 1295, 1305, and 2293 cm^{-1} . Gomes *et al.*³⁴ have also reported the similar experimental results. The present prediction is in good agreement with these observations. In Ref. 34, the authors have assigned the vibration at 1235 cm^{-1} to the second overtone of a librational mode. Our prediction suggests that this mode may be due to a first-order Raman process.

As shown in Fig. 4, the phonon frequencies are split into three separate regions, namely, region I: less than 500 cm^{-1} , region II: 1000 to 1300 cm^{-1} , and region III: 2250 to 2400 cm^{-1} .

The Li displacements are mainly involved the eigenmodes in the region I and are essentially negligible in the regions II and III. Analyzing the eigenvectors, we confirm that the eigenmodes in the regions II and III originate from the internal B-H bending and stretching vibrations of BH_4 complexes, respectively. For comparison, the vibrational frequen-

TABLE IV. Dielectric properties of orthorhombic LiBH₄. Macroscopic high- and low-frequency dielectric permittivity tensors ϵ_∞ and ϵ_0 , Born effective charge tensor Z^* .

	xx	yy	zz	xy	yz	zx	xz	zy	yx
ϵ_∞	2.37	2.49	2.36	0	0	0	0	0	0
ϵ_0	4.67	8.95	5.63	0	0	0	0	0	0
Z_{Li}^*	0.98	1.08	1.02	0	0	± 0.15	± 0.21	0	0
Z_{B}^*	0.10	0.15	0.06	0	0	± 0.12	± 0.11	0	0
Z_{H1}^*	-0.28	-0.18	-0.33	0	0	± 0.17	± 0.16	0	0
Z_{H2}^*	-0.32	-0.15	-0.41	0	0	± 0.12	± 0.12	0	0
Z_{H3}^*	-0.24	-0.45	-0.18	± 0.16	± 0.05	± 0.12	± 0.12	± 0.03	± 0.17

cies of a free $[\text{BH}_4]^{-1}$ anion are calculated.³⁵ The obtained frequencies and their symmetry labels for the point group T_d are 1029 (T_2) and 1154 (E) cm^{-1} for the bending modes, and 2225 (T_2) and 2236 (A_1) cm^{-1} for the stretching modes. The molecular approximation fairly reproduces the phonon frequencies in the regions II and III, implying strong internal bonding of BH_4 complexes.

Figure 5 shows the examples of the eigenmodes of orthorhombic LiBH₄ in the regions II and III. The internal B-H vibrations in Figs. 5(a) and 5(b) are clearly characterized as the E and A_1 modes of a free $[\text{BH}_4]^{-1}$ anion, respectively.

The eigenmodes in the region I are librational, which involve the displacements of both Li^+ cations and $[\text{BH}_4]^-$ anions. The infrared-active modes in this region are expected to yield considerable dipole-dipole interactions, which contribute the macroscopic low-frequency dielectric permittivity tensor ϵ_0 . The ionic contributions to ϵ_0 can decompose into that of each eigenmode [see Eq. (52) in Ref. 25]. This decomposition reveals that the contributions of the eigenmodes in region I to ϵ_0 are more than 96%. Unlike the internal vibrations of BH_4 complexes, the librational modes are thought to be sensitive to the crystal anisotropies, which will reflect the large anisotropies of ϵ_0 .

E. Formation energy

The heat of formation is the most fundamental and important quantity for the hydrogen storage materials. For LiBH₄, the cohesive energy and the zero-point energy is calculated

as 3.15 eV/atom and 178 meV/atom, respectively. Here, the zero-point energy is estimated from only the Γ -phonon eigenmodes. This treatment is justified by the fact that the molecular approximation is fairly good for the high-frequency internal bending and stretching modes of BH_4 complexes, which are expected to have the dominant contributions. Using these values and the energies given in Table I, the heat of formation for the reaction



is calculated. It is expected that the choice of the metastable α phase of B gives only minor effects because of the structural similarity with the ground state β -B, the same basic building blocks of an icosahedron. Considering only the total energies, the heat of formation is estimated as -194 kJ/mol. The heat of formation including the zero-point energies is -160 kJ/mol. The zero-point energies have moderate contributions. The experimental value¹¹ has been reported as -194 kJ/mol. The agreement of the heat of formation with the reported value is reasonably good when the zero-point energies are included. The excellent agreement without the zero-point energies is most likely accidental.

The following reaction is more closely related to the hydriding/dehydriding reactions:



The heat of formation for LiH is obtained as -153 (-162) kJ/mol H₂ with (without) the zero-point energy con-

TABLE V. Optical Γ -phonon frequencies (in cm^{-1}) of orthorhombic LiBH₄.

Modes	Frequencies										
A_g	107	196	229	280	432	1049	1200	1285	2292	2326	2368
B_{1g}	93	222	244	421	1047	1233	2347				
B_{2g}	165	248	269	340	411	1056	1206	1283	2294	2338	2382
B_{3g}	122	173	234	399	1052	1237	2344				
A_u	74	153	236	369	1043	1227	2345				
B_{1u} (TO)	163	249	344	390	1051	1203	1274	2293	2339	2359	
B_{1u} (LO)	166	344	345	421	1053	1211	1274	2295	2352	2365	
B_{2u} (TO)	175	195	342	1042	1234	2343					
B_{2u} (LO)	192	291	387	1050	1236	2374					
B_{3u} (TO)	217	256	331	367	1050	1206	1275	2294	2342	2366	
B_{3u} (LO)	217	291	361	409	1053	1210	1278	2297	2346	2384	

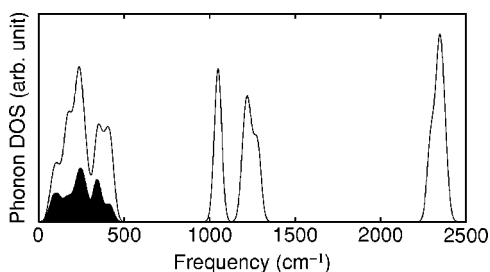


FIG. 4. Phonon density of states for orthorhombic LiBH_4 . The contribution of the optical Γ -phonon modes is only taken into account and the Gaussian broadening with a width of 30 cm^{-1} is used. The shaded parts indicate the partial density of states of Li, which is weighted by the norm of Li eigenvectors.

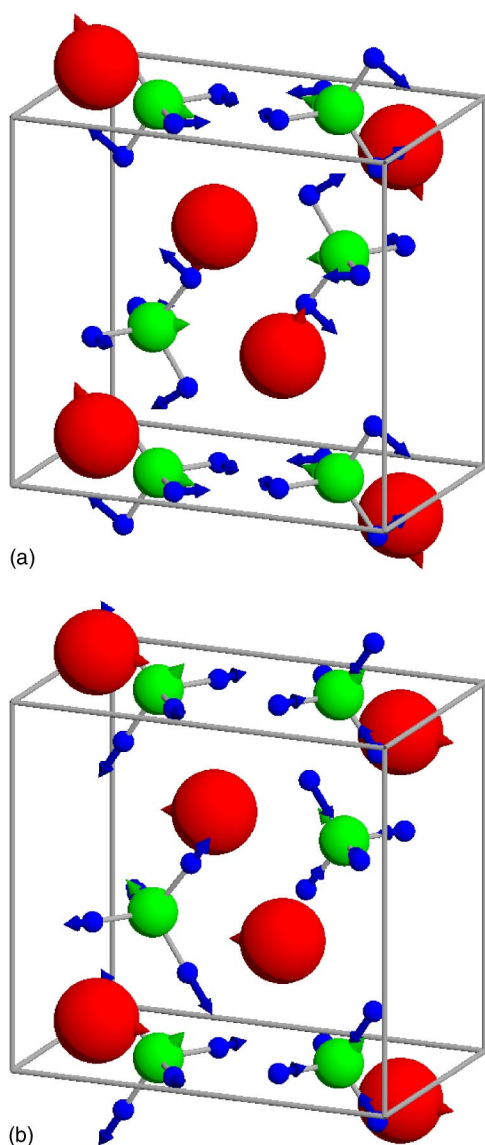


FIG. 5. (Color online) Optical Γ -phonon eigenmodes of orthorhombic LiBH_4 in (a) region II and (b) region III. The lengths of arrows correspond to the size of the eigendisplacements. See the caption of Fig. 1.

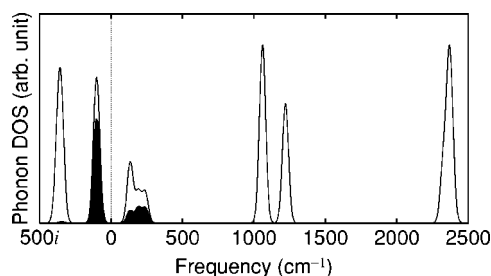


FIG. 6. Phonon density of states for hexagonal LiBH_4 . The TO-LO splitting is not taken into consideration. See the caption of Fig. 4.

tributions, which is in good agreement with the experimental value²⁹ of -157 kJ/mol H_2 . The heat of formation for Eq. (2) is predicted as -56 kJ/mol H_2 including the zero-point energies. The agreement with the experimental value¹¹ of -69 kJ/mol H_2 is reasonably good. Neglecting the zero-point energies, the predicted value becomes -75 kJ/mol H_2 .

F. Hexagonal phase at high temperature

The structural optimization gives a structure far away from the experimental configuration.¹² Li layers are located above BH_4 layers. Therefore, we fix the lattice constants and the positions of Li and B atoms and relax only the positions of H atoms, and then Li and B atoms are moved by hand using atomic forces as a guide. Starting from the experimental configuration, this optimization procedure is repeated until the maximum residual atomic force becomes less than 1×10^{-4} hartree/bohr. The total energy increases with decreasing the residual atomic forces during the optimization cycles, indicating that the final configuration is placed at the saddle point on the energy surface. The shape obtained for BH_4 complexes is very close to an ideal tetrahedron with the bond length of 1.23 \AA . The optimized position of B is $z = 0.629$ (Wyckoff notation, $2b$ site; the experimental value is $z = 0.553$). The interlayer distance between Li and BH_4 is somewhat larger than that in the experimental configuration.

The calculated Γ -phonon frequencies are shown in Fig. 6, in which the TO-LO splitting is not taken into account. There are seven soft modes which can be classified into two groups. One is located around $100i \text{ cm}^{-1}$, which contains three soft modes; $A_1 + E_1 + E_2$. The eigenvectors of the A_1 mode correspond to nearly rigid displacements of BH_4 layers along the c axis and displacements of Li layers in the opposite direction, by which the crystal symmetry is not changed. This soft mode is the origin of the structure far away from the experimental configuration given by the structural optimization described above. The E_1 and E_2 modes consist of sliding of Li layers against BH_4 layers. Another group is found around $300i \text{ cm}^{-1}$, suggesting more strong instability. The eigenvectors of 4 soft modes ($A_2 + B_2 + E_1 + E_2$) in this group correspond to nearly rigid rotations of BH_4 complexes. These modes are expected to be closely related to the dynamic disorder of BH_4 units in hexagonal LiBH_4 proposed by Gomes *et al.*³⁴ The finite temperature effects are probably crucial to study the structural properties in this phase.

The phonon frequencies originated from the internal B-H bending and stretching vibrations are almost same as those in the orthorhombic phase. The total and partial densities of states (not shown) are also very similar to those shown in Fig. 2. The bonding properties are not sensitive to the arrangements of Li atoms and BH_4 complexes. The obtained cohesive energy is 3.09 eV/atom which is slightly lower than that in the orthorhombic phase.

IV. SUMMARY

First-principles calculations have been performed on orthorhombic LiBH_4 to predict its fundamental properties. The calculation gives nearly an ideal tetrahedral configuration of BH_4 complexes although the recent experiment suggests that their configuration is strongly distorted. Analyses for the electronic structure and the Born effective charge tensors indicate that Li atoms are ionized as Li^+ cations. A boron atom constructs sp^3 hybrids and forms covalent bonds with surrounding four H atoms. A deficient electron to form these bonds is compensated by a Li^+ cation. The Γ -phonon frequencies originated from the internal B-H bending and stretching vibrations of BH_4 complexes can be fairly repro-

duced by the molecular approximation, suggesting the strong internal bonding of BH_4 . These bonding properties are expected to be held in the hexagonal phase observed at high temperature.

For practical applications, the destabilization of LiBH_4 to decrease the dehydriding temperature is an important research direction. From our results, it is expected that the charge compensation by Li^+ cations is a key feature for the stability of the internal bonding of $[\text{BH}_4]^-$ anions, and so the suppression of the charge transfer by the partial substitution of Li by other elements will be effective to lower the dehydriding temperature. The theoretical and experimental studies in this direction are now in progress for LiBH_4 and the related materials.

ACKNOWLEDGMENTS

We would like to thank T. Noritake, M. Aoki, G. Kitahara, T. Hioki, and A. Fukumoto for variable discussions. This study was partially supported by the New Energy and Industrial Technology Development Organization (NEDO), Basic Technology Development Project of Hydrogen Safety and Utilization (2002).

*Electronic address: miwa@cmp.tytlabs.co.jp

- ¹B. Bogdanović and M. Schwickardi, *J. Alloys Compd.* **253**, 1 (1997).
- ²R. A. Zidan, S. Takara, A. G. Hee, and C. M. Jensen, *J. Alloys Compd.* **285**, 119 (1999).
- ³L. Zaluski, A. Zaluuka, and J. O. Ström-Olsen, *J. Alloys Compd.* **290**, 71 (1999).
- ⁴K. J. Gross, S. Guthrie, S. Tanaka, and G. Thomas, *J. Alloys Compd.* **297**, 270 (1999).
- ⁵B. Bogdanović, R. A. Brand, A. Marjanović, M. Schwickardi, and J. Tölle, *J. Alloys Compd.* **302**, 36 (2000).
- ⁶C. M. Jensen and K. J. Gross, *Appl. Phys. A: Mater. Sci. Process.* **72**, 213 (2001).
- ⁷D. Sun, T. Kiyobayashi, H. Takeshita, N. Kuriyama, and C. M. Jensen, *J. Alloys Compd.* **337**, L8 (2002).
- ⁸G. P. Meisner, G. G. Tibbetts, F. E. Pinkerton, C. H. Olk, and M. P. Balogh, *J. Alloys Compd.* **337**, 254 (2002).
- ⁹G. Sandrock, K. Gross, and G. Thomas, *J. Alloys Compd.* **339**, 229 (2002).
- ¹⁰H. Morioka, K. Kakizaki, S.-C. Chung, and A. Yamada, *J. Alloys Compd.* **353**, 310 (2003).
- ¹¹A. Züttel, P. Wenger, S. Rentsch, P. Sudan, Ph. Mauron, and Ch. Emmenegger, *J. Power Sources* **118**, 1 (2003).
- ¹²J-Ph. Soulié, G. Renaudin, R. Černý, and K. Yvon, *J. Alloys Compd.* **346**, 200 (2002).
- ¹³P. Vajeeston, P. Ravindran, R. Vidya, H. Fjellvåg, and A. Kjekshus, *Phys. Rev. B* **68**, 212101 (2003).
- ¹⁴M. E. Arroyo y de Dompablo and G. Ceder, *J. Alloys Compd.* **364**, 6 (2004).
- ¹⁵D. Vanderbilt, *Phys. Rev. B* **41**, 7892 (1990); K. Laasonen, A. Pasquarello, R. Car C. Lee, and D. Vanderbilt, *ibid.* **47**, 10 142 (1993).

- ¹⁶P. Hohenberg and W. Kohn, *Phys. Rev.* **136** B864 (1964); W. Kohn and L. J. Sham, *ibid.* **140** A1133 (1965).
- ¹⁷J. P. Perdew, K. Burke, and M. Ernzerhof, *Phys. Rev. Lett.* **77**, 3865 (1996); **78**, 1396(E) (1997).
- ¹⁸D. D. Koelling and B. N. Harmon, *J. Phys. C* **10**, 3107 (1977).
- ¹⁹A. M. Rappe, K. M. Rabe, E. Kaxiras, and J. D. Joannopoulos, *Phys. Rev. B* **41**, 1227 (1990).
- ²⁰S. G. Louie, S. Froyen, and M. L. Cohen, *Phys. Rev. B* **26**, 1738 (1982).
- ²¹D. R. Hamann, M. Schlüter, and C. Chiang, *Phys. Rev. Lett.* **43**, 1494 (1979).
- ²²A. Fukumoto and K. Miwa, *Phys. Rev. B* **55**, 11 155 (1997).
- ²³K. Miwa and A. Fukumoto, *Phys. Rev. B* **65**, 155114 (2002).
- ²⁴N. Ohba, K. Miwa, N. Nagasako, and A. Fukumoto, *Phys. Rev. B* **63**, 115207 (2001).
- ²⁵X. Gonze and C. Lee, *Phys. Rev. B* **55**, 10 355 (1997).
- ²⁶K. Kunc and R. M. Martin, *Phys. Rev. Lett.* **48**, 406 (1982).
- ²⁷C. Kittel, *Introduction to Solid State Physics*, 6th ed. (Wiley, New York, 1986).
- ²⁸P. Villars and L. D. Calvert, *Pearson's Handbook of Crystallographic Data for Intermetallic Phases*, 2nd ed. (ASM International, Materials Park, Ohio, 1991).
- ²⁹Y. Fukai, *The Metal-Hydrogen System*, Vol. 21 of Springer Series in Material Science (Springer-Verlag, Berlin, 1993).
- ³⁰There are two independent atomic positions B1 and B2 (space group $R\bar{3}m$, Wyckoff notation, $18h$ site). The calculated positions are $(x, \bar{x}, z) = (0.119, -0.119, 0.109)$ and $(x, \bar{x}, z) = (0.136, -0.136, 0.358)$ for B1 and B2, and the experimental values are $(x, \bar{x}, z) = (0.120, -0.120, 0.110)$ and $(x, \bar{x}, z) = (0.133, -0.133, 0.363)$ for B1 and B2, respectively.
- ³¹T. Noritake, H. Nozaki, M. Aoki, S. Towata, A. Koiwai, E. Nishihori, M. Takata, and M. Sakata (private communication): Their

results are $d_{\text{B-H}}=1.11-1.19 \text{ \AA}$ and $\theta_{\text{H-B-H}}=103^\circ-113^\circ$.

³²A. Aguayo and D. J. Singh, Phys. Rev. B **69**, 155103 (2004).

³³Y. Nakamori and S. Orimo, J. Alloys Compd. **370**, 271 (2004).

³⁴S. Gomes, H. Hagemann, and K. Yvon, J. Alloys Compd. **346**,

206 (2002).

³⁵We use an fcc supercell with a lattice constant $a=12 \text{ \AA}$. The extra negative charge is compensated by the uniform background charge.